Journal of Photochemistry and Photobiology A: Chemistry 309 (2015) 1–7

Contents lists available at ScienceDirect

Journal of Photochemistry and Photobiology A: Chemistry

journal homepage: www.elsevier.com/locate/jphotochem

Ultrafast excited-state dynamics associated with the photoisomerization of *trans*-4-diethylaminoazobenzene in solution

Yaping Wang, Song Zhang *, Simei Sun, Kai Liu, Bing Zhang **

State Key Laboratory of Magnetic Resonance and Atomic and Molecular Physics, Wuhan Institute of Physics and Mathematics, Chinese Academy of Sciences, Wuhan 430071, China

ARTICLE INFO

Article history:
Received 24 December 2014
Received in revised form 15 April 2015
Accepted 20 April 2015
Available online 22 April 2015

ABSTRACT

The ultrafast dynamics of S_2-excited *trans*-4-diethylaminoazobenzene (*trans*-4-DEAAB) is investigated in solution by femtosecond transient absorption spectroscopy combined with quantum chemical calculations. Following excitation, the internal conversion from the S_2 state to the S_1 state occurs directly with time constant of ~0.10 ps. The *cis* isomer is observed by the partial recovery of ground-state bleach in 450–480 nm and the permanent positive absorption in 480–550 nm. The time constant of <1 ps is assigned to the lifetime of the S_1 state which decays by isomerization to the *cis*-isomer hot S_0 state and internal conversion to the *trans*-isomer hot S_0 state. The photoisomerization is deduced by inversion mechanism because of the independence between the viscosity and the S_1-state lifetime. The vibrational cooling of the hot S_0 state of *cis*-4-DEAAB occurs with ~15 ps in acetone but is shortened to ~6 ps in alcohols solvents. This shortening is due to the H-bond which forms easily in protic solvent and accelerates the flow of vibrational energy between solute and solvent.

1. Introduction

Azobenzene and its derivatives are widely applied in optical memory logical devices, molecular manipulators and photochromic molecular switches because their reversible E ⇄ Z photoisomerization can change molecular structure, dipole, absorption spectrum and dielectric constant [1–8]. In particular, azobenzene derivatives also exhibit a high potential in biological application [9–13], such as the artificial photocontrolled proteins [9] and the photoresponsive gene [10].

A diethylamino group substituted azobenzene, *trans*-4-diethylaminoazobenzene (*trans*-4-DEAAB) is of particular interest because of its para substitution of aminoethyl, which can attach to the interior position of DNA triplex. And the photoregulation is the most effective for *p*-aminoazobenzene types [14]. Comparing to azobenzene, the diethylamino group can result in a large red-shift of the $\pi\pi^*$ state which locates at ~410 nm [15]. The isomerization yield of the trans-4-DEAAB in apolar solvent is almost unity by irradiation in the visible region but reduces obviously in polar solvents [16]. These characters with the large photo-induced structural change determine the specific application of *trans*-4-DEAAB in photoelectrochemical information storage, nonlinear optics and photo-switchable gene [10,17,18]. To achieve these potential applications, it is necessary to have detailed knowledge about its ultrafast photoisomerization dynamics under different circumstances.

The photoisomerization dynamics of several amino group substituted azobenzene has also been investigated [19–22]. These studies show that the unusual roles of the first $n\pi^*$ and $\pi\pi^*$ states in the photoisomerization processes are apparently different due to substitution. Reid et al. observed that a bi-exponential decay behavior with time constants of ~0.8 ps and ~10 ps exists in the excited $\pi\pi^*$ state of *trans*-4-dimethylaminoazobenzene (*trans*-4-DMAAB) by a subpicosecond pump–probe spectroscopy [19]. The ~0.8-ps, and ~10-ps components are assigned to the lowest-lying $\pi\pi^*$ state and the isomerization, and the ground-state vibrational relaxation, respectively. However, Hirose et al. determined ultrafast photoisomerization dynamics of *trans*-4-aminoazobenzene (*trans*-4-AAB) in different solvent [20]. It is assumed that the $n\pi^*$ state is populated from the initially excited $\pi\pi^*$ state within 0.2 ps and then decays by isomerization to *cis* isomer and internal conversion to *trans*-isomer S_0 stated with time constant of ~0.6 ps and ~2 ps. It is unfortunately that the authors cannot distinguish the corresponding decay channels of these two time constants. For *trans*-4-DEAAB, the diethylamino group is proven to affect the energy of the $\pi\pi^*$ state [15]. The energetic ordering and roles of the first $n\pi^*$ and $\pi\pi^*$ in the photoisomerization and electronic deactivation processes is still unclear.

* Corresponding author. Tel.: +86 27 87198491; fax: +86 027 87198491.
** Corresponding author. Tel.: +86 27 87197441; fax: +86 027 87198491.
E-mail addresses: zhangsong@wipm.ac.cn (S. Zhang), bzhang@wipm.ac.cn (B. Zhang).

http://dx.doi.org/10.1016/j.jphotochem.2015.04.015
1010-6030/

In this paper, the ultrafast excited state dynamics and photoisomerization of *trans*-4-DEAAB, with the $\pi \rightarrow \pi^*$ excitation is investigated in ethanol, acetone and ethylene glycol by femtosecond transient absorption spectroscopy combined with quantum chemical calculations. The spectra are measured until the delay time up to 300 ps to obtain more complete information on the molecular dynamics. The quantum chemical calculations are used to present the energetic ordering, vertical excitation energies, oscillator strength and static absorption spectra of the *cis* and *trans* isomer. Following the excitation at 400 nm, ultrafast excited-state dynamics associated with the photoisomerization of *trans*-4-DEAAB are observed and analyzed in detail.

2. Experimental and computational details

Trans-4-DEAAB (98% purity) was purchased from Alfa Aesar, and used for experiments without further purification. Ethanol, acetone and ethylene glycol purchasing from Aladdin (99% purity) were used as solvents. All of them are polar solvents with viscosities of 1.2, 0.32 and 13.5 mPa s at 20 °C, respectively [23,24]. The concentration of *trans*-4-DEAAB in each solvent was 1 mM at room temperature and a fresh sample was prepared for each experiment. The static absorption spectra were conducted in a 1-mm quartz cell by the UV–vis spectrometer (INESA, L6) and normalized in all three solvents.

The apparatus used for ultrafast transient absorption measurements is based on a regeneratively amplified femtosecond laser system which has been already described in detail earlier [25]. Briefly, the 800 nm seed beam with repetition rate of 78 MHz is generated by a commercial Ti:sapphire oscillator. The seed beam is brought into the regenerative amplifier and the output used as fundamental pulse was set at repetition rate of 1 kHz, center wavelength of 800 nm, duration of 35 fs and the energy up to 1 mJ/pulse. The second harmonic generation of the fundamental pulse (400 nm) was generated by a 0.5 mm thick BBO crystal as the excitation light. The excitation intensity was set to less than 4 μJ/pulse for measurements. A portion of the fundamental pulse was focused into a 1 mm sapphire to generate a white continuum (450–690 nm). In order to correct the pulse-to-pulse intensity fluctuations and improve the measuring sensitivity, the white light was split into the probe and the reference beam by a metallic-coated beamsplitter. The polarization angle between the pump and probe beam is set at the magic angle (54.7°) for eliminating polarization and photoselection effects. The sample was contained in a flow cell with 0.2 mm quartz windows and 1 mm optical path length. The pump and probe pulses with an intersection angle of ~4° overlapped in the sample spatially, and the reference beam was focused on the sample at a different spot. The probe pulse was temporally delayed with respect to the pump pulse through a computer controlled translation stage. A CCD camera (PI-MAX, 1024 × 256 pixel array) equipped with a spectrometer (Princeton, SpectraPro 2500i) was used to collect the probe and reference beams. Each of the recorded spectra is accumulated on the CCD for typically 10000 laser shorts. The instrumental response of the system was determined to be ~0.17 ps by cross-correlation measurements between the pump and probe pulses. The cross-correlation measurements were also used to determine the precise zero time-delay at each probe wavelength. In order to eliminate any persistent offset in the optical density at long delay times, a time constant of 10,000 ps was included. The time evolutions of transient absorption data of *trans*-4-DEAAB for all three solvents were fitted by global fit analysis with singular value decomposition (SVD).

All quantum chemical calculations were carried out with the Gaussian 09 software package [26]. The molecular geometries in the electronic ground state of both *trans* and *cis*-4-DEAAB were optimized using ab initio density-functional theory with the B3LYP functional and the 6-311G++(d,p) basis set. All the minima are verified by vibrational frequency analysis at the same level of theory. The polarizable continuum model (PCM) was used to incorporate the bulk solvent effect [27]. The vertical transition energies, oscillator strengths and absorption spectroscopy were performed by the TD-DFT/B3LYP with the basis set of 6-31G in ethanol and acetone and 6-311G in ethylene glycol, respectively.

3. Results and discussion

3.1. Quantum chemical calculations

Table 1 shows the orbital transitions, configuration-interaction (CI) coefficients, vertical excitation energies, and oscillator strengths of the two lowest excited singlet states of *trans*-4-DEAAB in ethanol, acetone and ethylene glycol, respectively. For *trans*-4-DEAAB in ethanol, the first transition is from HOMO-1 to LUMO and the oscillator strength is zero, while the second transition from HOMO to LUMO is much more intense. The assignments of molecular orbitals are done by visual inspection. The HOMO-1, HOMO and LUMO are assigned to n, π and π^* orbitals, respectively, as shown in Fig. 1. Evaluation of molecular orbitals reveals that the first transition is of 99% $n \rightarrow \pi^*$ character from the CI coefficients while the second transition is of 100% $\pi \rightarrow \pi^*$ character. In acetone and ethylene glycol, the calculated results are the same as that in ethanol. It clearly demonstrates that the S_1 state is optically-forbidden with $n\pi^*$ character while the S_2 state is optically-allowed with $\pi\pi^*$ character.

3.2. Static absorption spectrum

The static absorption spectra of *trans*-4-DEAAB in ethanol, acetone and ethylene glycol were measured and shown in Fig. 2(a),

Table 1
Orbital transition, configuration-interaction (CI) coefficients, vertical excitation energy, and oscillator strength of the two lowest excited singlet states of *trans*-4-DEAAB in ethanol, acetone and ethylene glycol.

State	Orbital transition	CI coefficients	Vertical excitation/eV	Oscillator strengths
Ethanol				
S_1	HOMO-1 → LUMO	0.70531	2.51	0.0000
S_2	HOMO → LUMO	0.70709	2.97	1.1016
Acetone				
S_1	HOMO-1 → LUMO	0.70531	2.51	0.0000
S_2	HOMO → LUMO	0.70708	2.97	1.1003
Ethylene glycol				
S_1	HOMO-1 → LUMO	0.70500	2.57	0.0000
S_2	HOMO → LUMO	0.70662	2.90	1.1142

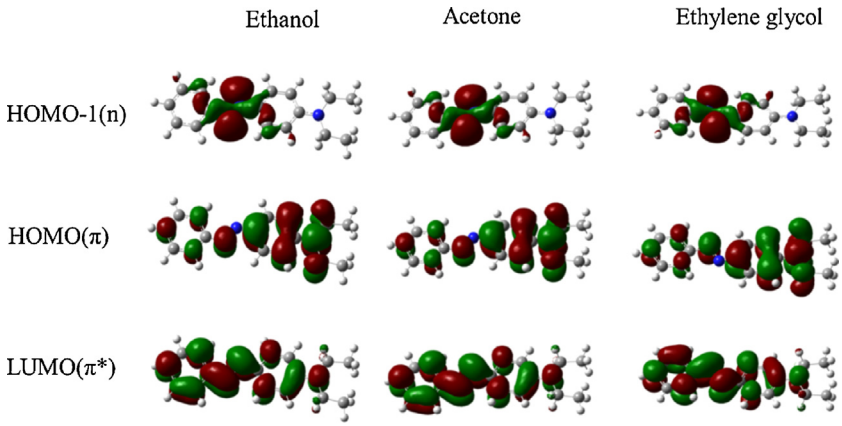

Fig. 1. Molecular orbital of HOMO-1, HOMO, and LUMO of *trans*-4-DEAAB in ethanol, acetone and ethylene glycol calculated by B3LYP/6-311G++(d,p).

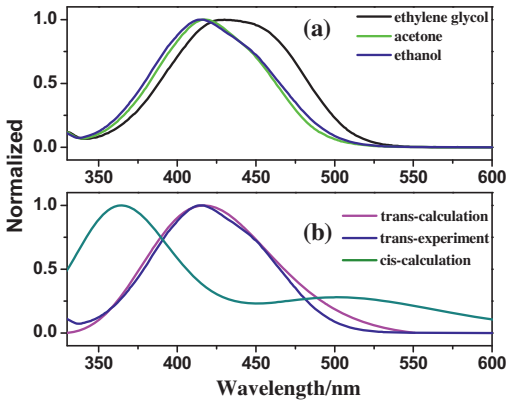

Fig. 2. (a) Static absorption spectra of *trans*-4-DEAAB in ethylene glycol (black), acetone (green) and ethanol (blue) by experiments. (b) Static absorption spectra of *trans* and *cis*-4-DEAAB by experiment and calculation in ethanol. (For interpretation of the references to color in this figure legend, the reader is referred to the web version of this article.)

respectively. All of them are dominated by a strongly allowed $\pi \rightarrow \pi^*$ (the S_2 state) transition with the center wavelengths of 416 nm in ethanol and acetone and 430 nm in ethylene glycol, respectively. A clear shoulder can be observed in 450–470 nm with a secondary intensity. For *trans*-azobenzene, the experimental value of oscillator strength of the $n\pi^*$ transition is measured to be the order of 10^{-2} [28] and larger than the calculated one [28,29]. For *trans*-4-DEAAB, the experimental value should be larger than that of azobenzene, because *trans*-4-DEAAB has lower symmetry than that of azobenzene without any substitution. Although the oscillator strength of the $n\pi^*$ transition of *trans*-4-DEAAB is calculated to be $<10^{-4}$, the shoulder in 450–470 nm is attributed to the $n\pi^*$ transition of *trans*-4-DEAAB which is hidden under the intense $\pi\pi^*$ band. Similar phenomenon can be observed in *trans*-4-AAB dissolved in ethanol [20] and 4-[*N*-ethyl-*N*-(2-hydroxyethyl)amino]-4′-nitro-azobenzene (DR1) dissolved in 2-fluorotoluene [30]. Fig. 2(b) shows the calculated and experimental absorption spectra of *trans*-4-DEAAB in ethanol. Both spectra are consistent well with each other. It indicates that our calculations are much accuracy. The absorption spectrum of *cis*-4-DEAAB in ethanol was also calculated at the same level and shown in

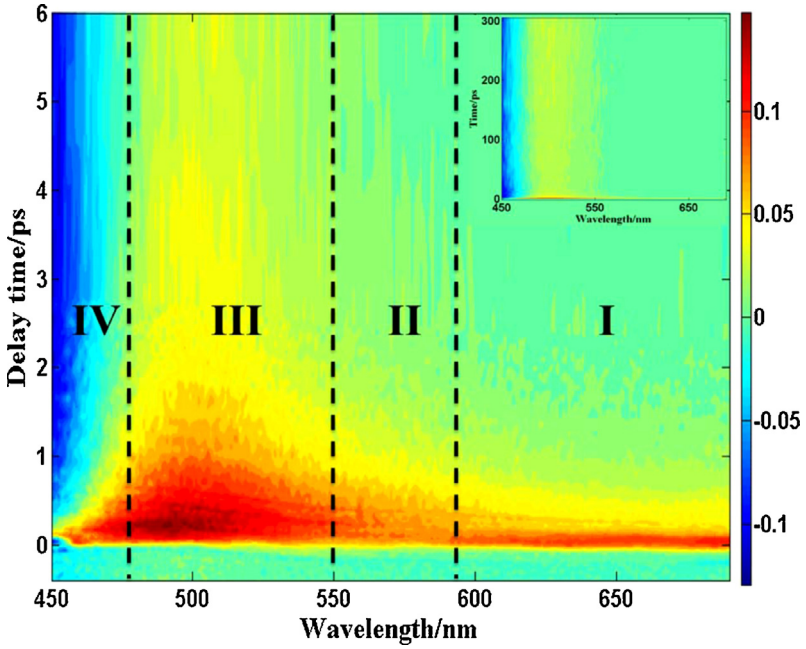

Fig. 3. Two-dimensional transient absorption spectrum of *trans*-4-DEAAB in ethanol with delay time to 6 ps and 300 ps (insert). The spectrum is divided into four distinctive regions of 590–690 nm (range I), 550–590 nm (range II), 480–550 nm (range III) and 450–480 nm (range IV).

Fig. 2(b). The absorption peaks of the S_1 and S_2 states of *cis*-4-DEAAB in ethanol are located at the 504 nm and 364 nm, respectively. It is similar with the experimental results performed by Allen and Binkley [15]. It shows that the two absorption peaks of the *cis* isomer in toluene locate in 500 nm and 350 nm, respectively. It is obviously that the first absorption band of the *cis* isomer locates in the range of 480–550 nm where the *trans* isomer absorbs very weak. The absorption spectra of *cis*-4-DEAAB in acetone and ethylene glycol were also calculated. The transitions to the S_1 state of *cis*-4-DEAAB in all solvents we used are not forbidden because of the broken symmetry. The calculated spectra are very similar to that in ethanol, which were not shown here anymore.

3.3. The excited-state dynamics of trans-4-DEAAB in ethanol

Fig. 3 displays the two-dimensional transient absorption spectrum of *trans*-4-DEAAB in ethanol with the delay time up to 6 ps in probe wavelengths of 450–690 nm. A full spectrum with delay time to 300 ps is also inserted in Fig. 3 and clearly shows that little change occurs after 6 ps. The spectrum shows four distinctive regions of 590–690 nm (range I), 550–590 nm (range II), 480–550 nm (range III) and 450–480 nm (range IV). The blue region in range IV is a negative signal and elucidated by the ground-state bleach. The significant ground-state bleach remains at the maximum delay time of 300 ps we measured. All the electronic and vibrational relaxation is finished in hundreds of picoseconds. This partial recovery of ground-state bleach reflects that photoisomerization of the *trans*-4-DEAAB occurs. The red regions in I, II and III are all the positive signal representing the excited-state absorption. It is noticed that there is a signal maintaining ~0.02 until the decay time up to 300 ps in the range III. The permanent signal is assigned to the *cis* isomer because the absorption of the S_1 state in *cis*-4-DEAAB locates exactly in this range. The transient spectra at selected delay times are displayed in Fig. 4. The upper panel (Fig. 4a) shows the ultrafast time evolution of absorption spectra within the first 300 fs after the excitation. The subsequent changes up to 300 ps are given in the lower panel (Fig. 4b). After exciting to the S_2 state by 400 nm, the absorption in the range I arises immediately and is clearly faster than that in 480–590 nm (Fig. 4a). The absorption in the range I has already reached its maximum at 76 fs, whereas the absorption in 480–590 nm is still at <30% of its eventual maxima. It indicates that the signal in the range I includes the excited S_2-state information. And then, the signal in the range I decrease with the increase of that in 480–590 nm which attains a maximum at 215 fs. This clearly indicates a direct dynamical conversion from one state into the other state. It can be deduced that the decay time of the S_2 state is ultrafast and close to an instrument-response limited. Fig. 4b shows that the positive signal in the whole spectral range decays within ~1.5 ps and maintain ~0.02 in 480–550 nm until the decay time up to 300 ps.

To properly describe the dynamics of *trans*-4-DEAAB in ethanol, global fit analysis of all of the kinetics at different wavelength regions is performed with singular value decomposition (SVD). Decay-associated difference spectra (DADS) with four time components were obtained from the global analysis, as shown in Fig. 5. The best fit results of the decay times and corresponding amplitudes are listed in Table 2. Several representative decay traces at selected probe wavelengths of *trans*-4-DEAAB in ethanol are shown in Fig. 6. The global analysis result shows a good match with the experimental traces over the whole spectra-temporal range. The DADS with lifetime of 0.11 ps presents the positive amplitudes longer than 600 nm and the negative amplitudes below the 600 nm. It is attributed to the S_2 state because the lifetime of the S_2 state is deduced to be ultrafast and close to an instrument-response limited above. Similar time scales of the S_2 state are obtained in azobenzene and other derivatives [20,30–33]. Hirose et al. assumed that the $n\pi^*$ state was populated by the initially excited $\pi\pi^*$ state of *trans*-4-AAB within ~0.2 ps [20]. Furthermore, Mayer et al. revealed that the isomerization occurs on the lowest-lying $\pi\pi^*$ state of *trans*-4-DMAAB with time constant of ~0.8 ps [19]. The excited S_2 state of *trans*-4-DEAAB with $\pi\pi^*$ character may decay by two channels. The first channel is the isomerization to the *cis* isomer and the second one is internal conversion to the *trans*-isomer S_1 state. The isomerization time of *trans*-azobenzene was proven to be 0.5–12.5 ps depending on the solvent [31,34,35]. The para-substitution may make the isomerization even more difficult because of the heavier phenyl. As the results, it is difficult that the isomerization complete in such fast 0.11 ps timescale. However, Fujino et al. concluded that the quantum yield of the $S_2 \rightarrow S_1$ electronic relaxation of *trans*-azobenzene is almost unity [34]. A diethylamino-substitution leads to a large red-shift of the $\pi\pi^*$ (S_2) state and makes the energy gap between $\pi\pi^*$ (S_2) and $n\pi^*$ (S_1) state much closer. The internal conversion from the S_2 to S_1 state should be easier. It is concluded that the internal conversion to the S_1 state is the appropriate channel of the S_2-state decay. The DADS with lifetime of 0.64 ps is positive at all wavelengths. The amplitude is relatively stronger under 600 nm. As mentioned above, the increase of S_1 state is accompanied by the decrease of S_2 state. The character in spectra of

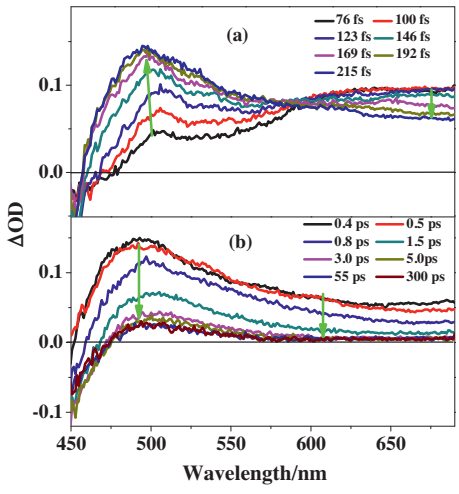

Fig. 4. Transient spectra of *trans*-4-DEAAB in ethanol at different delay times within 215 fs (a) and between 0.4 ps ≤ Δ*t* ≤300 ps (b) after the pump pulse at 400 nm. The arrows indicate the temporal evolution of the transient spectra.

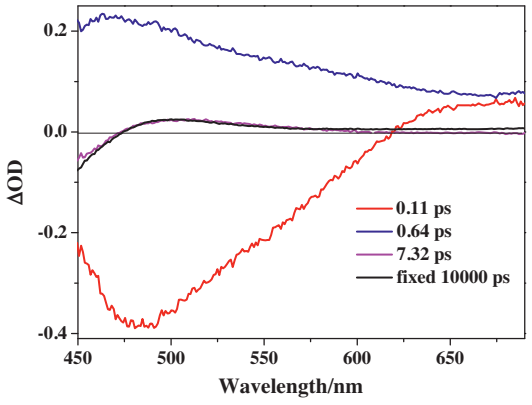

Fig. 5. Decay-associated difference spectra (DADS) of the four time constants extracted from the transient absorption data after SVD/global fit analysis.

Table 2
Results of the global fit analysis of the absorption–time profiles of *trans*-4-DEAAB in ethanol. Values in parentheses give the standard error.

λ_{Probe}[a] (nm)	a_1	τ_1 (ps)	a_2	τ_2 (ps)	a_3	τ_3 (ps)	a_4	τ_4[b] (ps)
680	0.97(0.08)	0.11(0.02)	0.55(0.04)	0.64(0.10)	−0.02(0.02)	7.32(0.80)	0.08(0.01)	Fixed
660	1.04(0.08)	0.11(0.02)	0.63(0.04)	0.64(0.10)	−0.01(0.02)	7.32(0.80)	0.06(0.01)	Fixed
640	0.93(0.08)	0.11(0.02)	0.73(0.04)	0.64(0.10)	−0.01(0.02)	7.32(0.80)	0.07(0.01)	Fixed
620	0.46(0.08)	0.11(0.02)	0.86(0.04)	0.64(0.10)	−0.01(0.02)	7.32(0.80)	0.04(0.01)	Fixed
570	−0.94(0.22)	0.11(0.02)	1.25(0.06)	0.64(0.10)	0.12(0.02)	7.32(0.80)	0.06(0.01)	Fixed
550	−0.38(0.24)	0.11(0.02)	1.18(0.06)	0.64(0.10)	0.10(0.02)	7.32(0.80)	0.08(0.01)	Fixed
530	−0.67(0.18)	0.11(0.02)	1.17(0.06)	0.64(0.10)	0.14(0.02)	7.32(0.80)	0.10(0.01)	Fixed
510	−0.92(0.18)	0.11(0.02)	1.14(0.04)	0.64(0.10)	0.17(0.02)	7.32(0.80)	0.13(0.01)	Fixed
500	−0.98(0.14)	0.11(0.02)	1.12(0.04)	0.64(0.10)	0.18(0.02)	7.32(0.80)	0.11(0.01)	Fixed
490	−0.75(0.08)	0.11(0.02)	1.07(0.04)	0.64(0.10)	0.14(0.02)	7.32(0.80)	0.09(0.01)	Fixed

[a] Wavelength at which the transient change in optical density was measured.
[b] A time constant of 10,000 ps was included to correspond to the permanent photoproduct in the optical density at long delay times.

the 0.64-ps component is consistent with that of S_1 state shown in Fig. 4. This 0.64-ps component therefore is considered from the contribution of S_1 state. Albini et al. concluded the isomerization yield of *trans*-4-DEAAB in a polar solvent (cyclohexane) is almost unity by irradiation of 434 nm but reduces obviously in polar solvents (alcohols) [16]. In our experiment, ethanol, acetone and ethylene glycol belong to the polar and are used as solvents, respectively. The isomerization yield of *trans*-4-DEAAB in these polar solvents did not reach to unity. As the result, the S_1 state decays by internal conversion to the *trans*-isomer S_0 state and isomerization to the *cis*-isomer hot S_0 state. The shape of the DADS with lifetime of 7.32 ps is similar to that with longtime constant of fixed 10,000 ps. Both of them show that the main absorption is located in the 480–550 nm. It exactly corresponds to the static absorption band of the S_1 state of *cis*-4-DEAAB. The component with 7.32 ps is attributed to the vibration cooling of the hot S_0 state of *cis* isomer whereas the longtime constant is originated from the *cis* isomer.

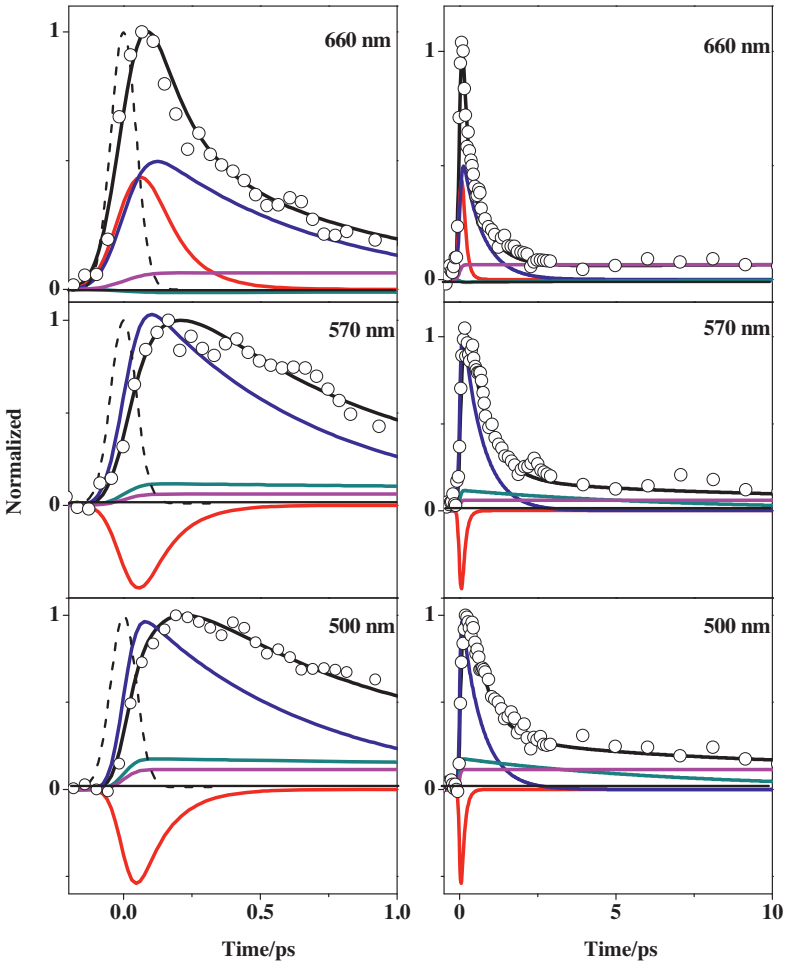

Fig. 6. Representative time traces of the transient absorption spectra of *trans*-4-DEAAB recorded upon excitation at 400 nm in ethanol for delay times up to Δt = 1.0 ps (left column) and Δt = 10 ps (right column). Open circles are data; solid black lines are the overall least-squares fit curves. The different contributions are indicated by colored lines (red: 0.11 ps; blue: 0.64 ps; dark cyan: 7.32 ps; magenta: 10,000 ps. The thin dashed curves on the left show the IRF. (For interpretation of the references to color in this figure legend, the reader is referred to the web version of this article.)

Table 3
Lifetimes obtained from global fit analysis of the transient absorption data of *trans*-4-DEAAB in three solvents. Values in parentheses give the standard error.

Solvent	Vscosity (mPa s)[a]	τ_1 (ps)	τ_2 (ps)	τ_3 (ps)	τ_4[b] (ps)
Ethanol	1.2	0.11(0.02)	0.64(0.10)	7.32(0.80)	Fixed
Acetone	0.32	0.06(0.02)	0.65(0.10)	15.0(0.90)	Fixed
Ethylene glycol	13.5	0.10(0.02)	0.92(0.12)	5.64(0.70)	Fixed

[a] Solvent viscosity at 20 °C obtained in Ref. [24].
[b] A time constant of 10,000 ps was included to correspond to the permanent photoproduct in the optical density at long delay times.

3.4. Solvent effects

The excited-state dynamics of *trans*-4-DEAAB have also been studied in acetone and ethylene glycol. Global analysis results are preformed and as similar as that in ethanol. All the time constants are listed in Table 3. All the S_2-state lifetimes in these three solvents are ultrafast. There is almost no change of the S_1-state lifetime although the viscosity is much different of ethanol, acetone and ethylene glycol. The independence of the solvent viscosity and the S_1-state lifetime indicates that the photoisomerization on the S_1 state is not by the rotation mechanism but by the inversion mechanism. It is reasonable that the effect of the solvent viscosity is weaker on the inversion process than the rotation process because of the smaller change of the volume in the inversion process. For example, solvent viscosity has a strong effect on the timescale of the photoisomerization in *trans*-stilbene, whose isomerization occurs by rotation process [36]. The decay time τ_3 is assigned to the lifetime of the vibrational cooling in *cis*-isomer S_0 state and determined to be 15.0 ps in acetone, 7.32 ps in ethanol and 5.64 ps in ethylene glycol, respectively. Obviously, it is faster in alcohols than that in acetone. As we known, the solute including a highly electronegative atom can attract hydrogen of the protic solvent to form H-bond. The H-bond between solvent and solute can transfer the excess vibrational energy to the environment extremely rapidly and result in the fast intermolecular vibration relaxation [37]. It is clearly that the vibrational cooling of the *cis*-isomer S_0 state is faster in alcohols than that in acetone, since highly electronegative atom N in *cis*-4-DEAAB can attract hydrogen from alcohols solvent.

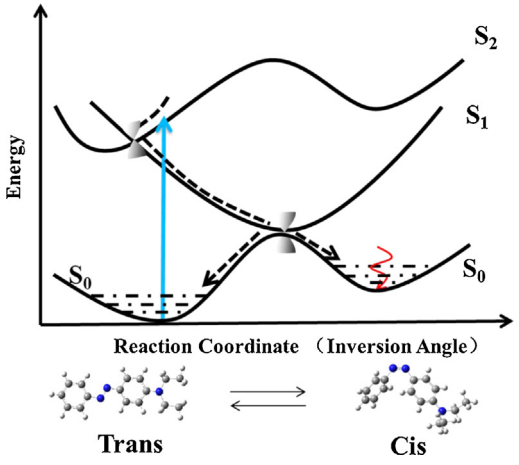

Fig. 7. The general photoinduced mechanisms for the S_2-excited *trans*-4-DEAAB.

4. Conclusion

In this paper, the ultrafast excited-state dynamics associated with the photoisomerization of a substituted *trans*-azobenzene, *trans*-4-DEAAB with the $\pi \rightarrow \pi^*$ excitation is investigated in ethanol, acetone and ethylene glycol by femtosecond transient absorption spectroscopy and quantum chemical calculations. According to calculations, the $n\pi^*$ state is the lowest excite state with oscillator strength of zero whereas the $\pi\pi^*$ state is optically-allowed. Following the photoexcitation, the internal conversion from the S_2 state to the S_1 state occurs directly with ultrafast timescale. The *cis* isomer is observed by the partial recovery of ground-state bleach in 450–480 nm and the permanent positive absorption in 480–550 nm. The photoisomerization evolves on the S_1 state potential energy surface and is deduced by inversion mechanism because of the independence between the viscosity and the S_1-state lifetime. The vibrational cooling of the hot S_0 state of *cis*-4-DEAAB occurs with ~15 ps in acetone but is shortened to ~6 ps in alcohols solvents. This shortening is due to the H-bond which forms easily in protic solvent and accelerates the flow of vibrational energy between solute and solvent. A general photoinduced mechanism for the S_2-excited *trans*-4-DEAAB is drawn in Fig. 7.

Acknowledgements

This work was supported by the National Basic Research Program of China (Grant No. 2013CB922200) and the National Natural Science Foundation of China (Grant Nos. 11174328, 21173256, and 21203241, 91121006, and 21273274).

References

[1] H. Rau, Photochromism: Molecules and Systems, Elsevier, Amsterdam, 1990 (Chapter 4).
[2] T. Ikeda, O. Tsutsumi, Optical switching and image storage by means of azobenzene liquid-crystal films, Science 268 (1995) 1873–1875.
[3] Z. Sekkat, M. Dumont, Photoassisted poling of azo dye doped polymeric films at room temperature, Appl. Phys. 54 (1992) 486–489.
[4] A. Natansohn, P. Rochon, Photoinduced motions in azo-containing polymers, Chem. Rev. 102 (2002) 4139–4175.
[5] L. Ulysse, J. Cubillos, J. Chmielewski, Photoregulation of cyclic peptide conformation, J. Am. Chem. Soc. 117 (1995) 8466–8467.
[6] K.G. Sudesh, D.C. Neckers, Photochemistry of azobenzene-containing polymers, Chem. Rev. 89 (1989) 1915–1925.
[7] D.G. Flint, J.R. Kumita, O.S. Smart, G.A. Woolley, Using an azobenzene cross-linker to either increase or decrease peptide helix content upon *trans*-to-*cis* photoisomerization, Chem. Biol. 9 (2002) 391–397.
[8] S. Spörlein, H. Carstens, H. Satzger, C. Renner, R. Behrendt, L. Moroder, P. Tavan, W. Zinth, J. Wachtveitl, Ultrafast spectroscopy reveals subnanosecond peptide conformational dynamics and validates molecular dynamics simulation, Proc. Natl. Acad. Sci. 99 (2002) 7998–8002.
[9] G.A. Woolley, Photocontrolling peptider α helices, Acc. Chem. Res. 38 (2005) 486–493.
[10] X.G. Liang, K. Fujioka, Y. Tsuda, R. Wakuda, H. Asanuma, Construction of a photo-switchable gene for turning on and off gene expression with light irradiation, Nucleic Acids Symp. Ser. 52 (2008) 19–20.
[11] C. Dohno, S. Uno, K. Nakatani, Photoswitchable molecular glue for DNA, J. Am. Chem. Soc. 129 (2007) 11898–11899.
[12] T. Chen, A. Yamaguchi, K. Igarashi, N. Igarashi, H. Nishioka, H. Asanuma, M. Yamashita, Ultrafast photoisomerization and its single-shot pump pulse efficiency of *trans*-azobenzene derivative: compound for photosensitive DNA, Opt. Commun. 285 (2012) 1206–1211.
[13] S. Dong, M. Löweneck, T. Schrader, W. Schrader, W. Zinth, L. Moroder, C. Renner, A photocontrolled β-hairpin peptide, Chem. Eur. J. 12 (2006) 1114–1120.
[14] X. Liang, H. Asanuma, M. Komiyama, Photoregulation of DNA triplex formation by azobenzene, J. Am. Chem. Soc. 124 (2002) 1877–1883.
[15] N.S. Allen, J.P. Binkley, A laser flash photolysis study of 4-*N*,*N*-diethylamino-azobenzene in solution: influence of epoxy resin, J. Photochem. 26 (1984) 213–220.
[16] A. Albini, E. Fasani, S. Pietra, The photochemistry of azo dyes. Photoisomerisation versus photoreduction from 4-diethylaminoazobenrene and 4-diethylamino-4′-methoxyazobenzene, J. Chem. Soc. Perkin Trans. 2 (1983) 1021–1024.

[17] Z.F. Liu, K. Hashimoto, A. Fujishima, Photoelectrochemical information storage using an azobenzene derivative, Nature 347 (1990) 658–660.
[18] J. Martinez-Perdiguero, Y. Zhang, C. Walker, J. Etxebarria, C.L. Folcia, J. Ortega, M.J. O'Callaghan, U. Baumeister, Second harmonic generation in laterally azo-bridged H-shaped ferroelectric dimesogens, J. Mater. Chem. 20 (2010) 4905–4909.
[19] S.G. Mayer, C.L. Thomsen, M.P. Philpott, P.J. Reid, The solvent-dependent isomerization dynamics of 4-(dimethylamino) azobenzene (DMAAB) studied by subpicosecond pump–probe spectroscopy, Chem. Phys. Lett. 314 (1999) 246–254.
[20] Y. Hirose, H. Yui, T. Sawada, Effect of potential energy gap between the $n\pi^*$ and the $\pi\pi^*$ state on ultrafast photoisomerization dynamics of an azobenzene derivative, J. Phys. Chem. A 106 (2002) 3067–3071.
[21] Y.P. Wang, S. Zhang, S.M. Sun, K. Liu, B. Zhang, Ultrafast excited state dynamics of *trans*-4-aminoazobenzene studied by femtosecond transient absorption spectroscopy, Chin. J. Chem. Phys. 26 (2013) 651–655.
[22] L. Wang, J. Xu, H. Zhou, C. Yi, W. Xu, *Cis*-transisomerization mechanism of 4-aminoazobenzene in the S_0 and S_1 states: a CASSCF and DFT study, J. Photochem. Photobiol. A 205 (2009) 104–108.
[23] C. Reichardt, Solvatochromic dyes as solvent polarity indicators, Chem. Rev. 94 (1994) 2319–2358.
[24] M.A. Haidekker, T.P. Brady, D. Lichlyter, E.A. Theodorakis, Effects of solvent polarity and solvent viscosity on the fluorescent properties of molecular rotors and related probes, Bioorg. Chem. 33 (2005) 415–425.
[25] S. Sun, S. Zhang, K. Liu, Y. Wang, B. Zhang, The geometry relaxation and intersystem crossing of quaterthiophene studied by femtosecond spectroscopy, Photochem. Photobiol. Sci. 14 (2015) 853–858.
[26] M.J. Frisch et al., GAUSSIAN 09, Revision A.02, (2009).
[27] J. Tomasi, M. Persico, Molecular interactions in solution: an overview of methods based on continuous distributions of the solvent, Chem. Rev. 94 (1994) 2027–2094.
[28] T. Cusati, G. Granucci, E. Martínez-Núñez, F. Martini, M. Persico, S. Vázquez, Semiempirical Hamiltonian for simulation of azobenzene photochemistry, J. Phys. Chem. A 116 (2012) 98–110.
[29] I. Conti, M. Garavelli, G. Orlandi, The different photoisomerization efficiency of azobenzene in the lowest $n\pi^*$ and $\pi\pi^*$ singlets: the role of a phantom State, J. Am. Chem. Soc. 130 (2008) 5216–5230.
[30] M. Poprawa-Smoluch, J. Baggerman, H. Zhang, H.P.A. Maas, L.D. Cola, A.M. Brouwer, Photoisomerization of disperse red 1 studied with transient absorption spectroscopy and quantum chemical calculations, J. Phys. Chem. A 110 (2006) 11926–11937.
[31] T. Fujino, S.Y. Arzhansev, T. Tahara, Femtosecond/picosecond time-resolved spectroscopy of *trans*-azobenzene: isomerization mechanism following S_2 $(\pi\pi^*) \leftarrow S_0$ photoexcitation, Bull. Chem. Soc. Jpn. 75 (2002) 1031–1040.
[32] J. Bahrenburg, K. Röttger, R. Siewertsen, F. Renth, F. Temps, Sequential photoisomerisation dynamics of the push–pull azobenzene disperse red 1, Photochem. Photobiol. Sci. 11 (2012) 1210–1219.
[33] J. Azuma, N. Tamai, A. Shishido, T. Ikeda, Femtosecond dynamics and stimulated emission from the S_2 state of a liquid crystalline *trans*-azobenzene, Chem. Phys. Lett. 288 (1998) 77–88.
[34] T. Fujino, S.Y. Arzhantsev, T. Tahara, Femtosecond time-resolved fluorescence study of photoisomerization of *trans*-azobenzene, J. Phys. Chem. A 105 (2001) 8123–8129.
[35] H. Satzger, S. Spörlein, C. Root, J. Wachtveitl, W. Zinth, P. Gilch, Fluorescence spectra of *trans*- and *cis*-azobenzene-emission from the Franck–Condon state, Chem. Phys. Lett. 372 (2003) 216–223.
[36] D.H. Waldeck, Photoisomerization dynamics of stilbenes, Chem. Rev. 91 (1991) 415–436.
[37] M. Terazima, Vibrational relaxation from electronically photoexcited states in solution studied by the acoustic peak delay method: hydrogen bonding effect to betaine-30, Chem. Phys. Lett. 305 (1999) 189–196.